SCIENTIFIC REPORTS
nature research

OPEN

Surface modification of multilayer $FePS_3$ by Ga ion irradiation

Heng Xu[1], ShangWu Wang[1], JianMing Ouyang[1], Xin He[1], Hao Chen[2], YuBo Li[3], Yun Liu[4], Rui Chen[5] & JunBo Yang[1*]

In order to investigate the modification of the surface structure of $FePS_3$ via Ga^+ ion irradiation, we study the effect of thickness and Raman spectrum of multilayer $FePS_3$ irradiated for 0 μs, 30 μs, and 40 μs, respectively. The results demonstrate that the intensity ratio of characteristic Raman peaks are obviously related to the thickness of $FePS_3$. After Ga^+ ion irradiation, the $FePS_3$ sample gradually became thinner and the E_u peak and $Eg(v_{11})$ peak in the Raman spectrum disappeared and the peak intensity ratio of $A_{1g}(v_2)$ with respect to $A_{1g}(v_1)$ weakened. This trend becomes more apparent while increasing irradiation time. The phenomenon is attributed to the damage of bipyramid structure of $[P_2S_6]^{4-}$ units and the cleavage of the P-P bands and the P-S bands during Ga^+ ion irradiation. The results are of great significance for improving the two-dimensional characteristics of $FePS_3$ by Ga^+ ion beam, including structural and optical properties, which pave the way of surface engineering to improve the performance of various two-dimensional layered materials via ion beam irradiation.

Since the successful study of graphene, various types of two-dimensional (2D) layered materials (e.g. transition metal dichalcogenides (TMDCs), black phosphorus (BPs), and hexagonal boron nitride (hBN)) have attracted enormous interests due to their unprecedented physical properties[1–4]. Recently, 2D layered transition metal phosphorus trichalcogenides (MPS_3, M = Fe, Mn, etc.) have received enormous attentions[5–8]. As a member of MPS_3 family, $FePS_3$ is expected to be achieved by mechanical exfoliation method owning to its weak inter-layers van der Waals forces[9]. Due to its higher in-plane stiffness and lower cleavage energies than graphite, the bulk structure of $FePS_3$ could be exfoliated down to the atomic thickness. Consequently, the technique of ion beam modification to achieve desired properties of various materials has been rapidly developed[10–14]. There are three effects of ion beam irradiation on 2D materials: doping effect, structural modification and defect engineering[15,16]. Generally, dopants could increase the carrier mobility while defects could decrease resistivity of materials after irradiation. Different from electron beam irradiation, ion beam irradiation has more artificially controlled conditions, such as ion species, ion energies and beam intensity[15]. In recent years, a large amount of works have focused on the changes in the properties of 2D materials through ion beam irradiation. For instance, the multilayer graphene modified low-energy (1 keV) Ar ion beam irradiation is used to study the damage and oxidation processes[16]. The insulating defect line on the monolayer graphene obtained by high-energy (30 keV) Ga^+ ion beam corrosion is used to investigate its electrical behavior[17]. The Hall mobility of monolayer graphene also change when exposed to high-energy (35 keV) carbon ion irradiation[18]. In addition, Wang *et al.* studied the effects of surface modification of graphene induced by Ga^+ ion beam irradiation with varying dwell times and got many meaningful results[19]. Despite the fact that there are numerous achievements and research on ion modification, the majority of the materials modified by ion beam have been focused on the graphene, and the investigate of $FePS_3$ are rare. In particular, the influences of ion beam irradiation on the surface modification of $FePS_3$ have not been reported yet.

Herein, we focus on investigating the surface modification of multilayer $FePS_3$ via irradiating with Ga^+ ion beam under different irradiation times. Firstly, the $FePS_3$ samples are characterized by using optical microscopy, Raman spectroscopy, atomic force microscopy (AFM) and scanning electron microscope (SEM). Secondly, we study the corresponding relation between the intensity of characteristic peaks and the thicknesses of multilayer $FePS_3$. Thirdly, the samples with different thicknesses were irradiated by Ga^+ ion beam via employing focused ion beam system (FIB) with varying irradiation time, and then the changes of intensity of Raman characteristic signals are analyzed. Finally, the changes of material surface morphology after Ga^+ ion beam irradiation are

[1]Department of Physics, National University of Defense Technology, Changsha, 410072, China. [2]College of Physics and optoelectronic engineering, Shenzhen University, Shenzhen, 518000, China. [3]Department of Mathematics, National University of Defense Technology, Changsha, 410072, China. [4]College of Physics and Electronics, Hunan University, Changsha, 410006, China. [5]Department of Biology and Chemistry, National University of Defense Technology, Changsha, 410072, China. *email: yangjunbo@nudt.edu.cn

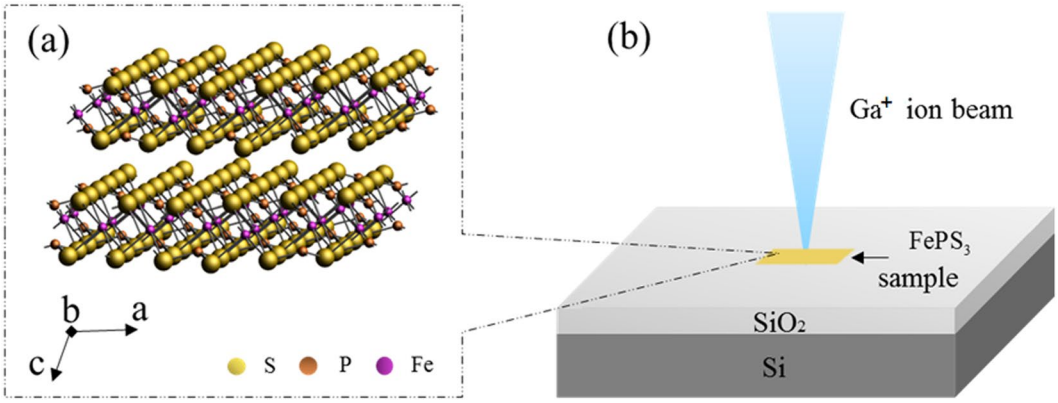

Figure 1. (**a**)The scheme of crystal $FePS_3$ structure; (**b**) Schematic illustration of $FePS_3$ irradiated by Ga^+ ion beam.

investigated by comparing the vibration modes of each peak. The results of this work are of great significance to explore the material properties of $FePS_3$ by Ga^+ ion modification.

Results

Preparation and characterization of $FePS_3$. The multilayer $FePS_3$ samples are prepared by mechanical exfoliation from bulk $FePS_3$ and then transferred onto the Si substrate with 300 nm thick SiO_2. As shown in Fig. 1(a), $FePS_3$ crystal has the $CdCl_2$ type-structure, in which Fe atoms are coordinated with six S atoms, P atoms are bonded to three S atoms, and Fe atoms and S atoms are not connected by any bonds[20]. Two P atoms and six S atoms form $[P_2S_6]^{4-}$ units of a bipyramid shape. Fe atoms and P atoms are sandwiched between S atoms layers to form the layer-shaped $FePS_3$ monoclinic symmetrical C2/m structure[9]. The lattice parameters are that a = 5.947 Å, b = 10.300 Å, c = 6.7222 Å, and $\beta = 107.16°$[21]. Optical microscope is used to identify the $FePS_3$ materials. Figure 2(a–f) show the optical image, SEM image, Raman spectra, AFM image and the thickness of sample, respectively. Raman spectroscopy is one of the most used non-destructive characterization techniques to study the properties of 2D materials. We utilize the Raman spectroscopy at room temperature with laser excitation wavelength of 785 nm. The Raman vibration modes of $FePS_3$ arise from two parts of the crystal structure, corresponding to the Fe atoms and the $[P_2S_6]^{4-}$ units[22]. The peaks of $FePS_3$ in Raman spectrum are attributed to vibration of $[P_2S_6]^{4-}$ units at room temperature. There exist three in-plane modes, E_g-type modes (depolarized, $E_g(\nu_{11}-\nu_{13})$), and three out-of-plane modes, A_{1g}-type modes (polarized, $A_{1g}(\nu_1-\nu_3)$), from the vibrations of the $[P_2S_6]^{4-}$ units, respectively[23]. When the $FePS_3$ samples are multilayers and the $[P_2S_6]^{4-}$ unit cell is doubled along the c axis, the out-of-plane vibration of two $[P_2S_6]^{4-}$ units in contiguous layers becomes Raman active and the E_u-type mode appears[23]. In general, the high-frequency peaks are mostly attributed to the molecular-like vibrations from $[P_2S_6]^{4-}$ bipyramid structures, while the low-frequency modes are put down to vibrations including Fe atoms. Considering lower energy of laser wavelength of 785 nm, only E_u peak at ~155 cm^{-1}, $E_g(\nu_{11})$ peak at ~277 cm^{-1}, $A_{1g}(\nu_1)$ peak at ~367 cm^{-1} and $A_{1g}(\nu_2)$ peak at ~246 cm^{-1} are measured in the Raman spectrum. Other Raman active modes could be obtained by using different excitation wavelengths (such as 488 nm and 514 nm). In our experiment, the Ga^+ ion beam irradiation is conducted using a FIB system with a kinetic energy of 30 keV and a beam current of 40 pA (at a fluence of ~2×10^{15} cm^{-2}). The size of the irradiated areas is about 10 μm × 10 μm. Before irradiation process, $FePS_3$ samples with different thickness are characterized using Raman spectroscopy and AFM. The AFM measurement are performed in the tapping mode of the scanning probe system to avoid additional damage for samples. Then the samples are irradiated by Ga^+ ion beam for 30 μs and 40 μs, respectively.

Experimental Results

$FePS_3$ samples with different thicknesses are obtained by mechanical exfoliation method. Figure 3(a) is the Raman spectra of samples, which shows that the relative peak intensity of all material characteristic peaks increases with the thickness of samples increasing in the normalized Raman spectrum. The E_u peak and the $E_g(\nu_{11})$ peak disappear when the thickness of the material is about 23 nm and the $A_{1g}(\nu_1)$ peak and $A_{1g}(\nu_2)$ peak exist though the intensity is weak. When the thickness of the sample is near 100 nm, the intensity of the $A_{1g}(\nu_1)$ peak is the same as the $A_{1g}(\nu_2)$ peak, indicating that the Raman activity of the two vibration modes are at a same level. When the thickness is increased to 230 nm, the intensity of the $E_g(\nu_{11})$ peak is equal to that of the substrate material *Si-2TA(x)* at ~302 cm^{-1}. In order to establish the corresponding relationship of the relative intensity of each peak and the intensity ratio of the peak as a function of thickness, we select the peak intensity values of the $A_{1g}(\nu_1)$, $A_{1g}(\nu_2)$ and *Si-2TA(x)* peaks as the main parameters to investigate the effect of Ga^+ irradiation with different irradiation times. As shown in Fig. 3(b), the curve is the intensity ratio versus the thickness of samples. When decreasing the thickness of samples, the intensity of the out of plane modes is increased. The intensity ratio of $A_{1g}(\nu_2)$ with respect to *Si-2TA(x)* peaks maintains a sustained and rapid upward trend with thickness, the value of which reaches to 1.807 at 230 nm. Besides this, the intensity ratio of $A_{1g}(\nu_1)$ with respect to *Si-2TA(x)* peaks also keeps going up and increases from 0.379 at ~25 nm to 1.812 at ~225 nm. We find that the intensity ratio of $A_{1g}(\nu_2)$ with respect to $A_{1g}(\nu_1)$ peaks decline with thickness, from 1.162 at 25 nm to 0.953 at 100 nm. And then the

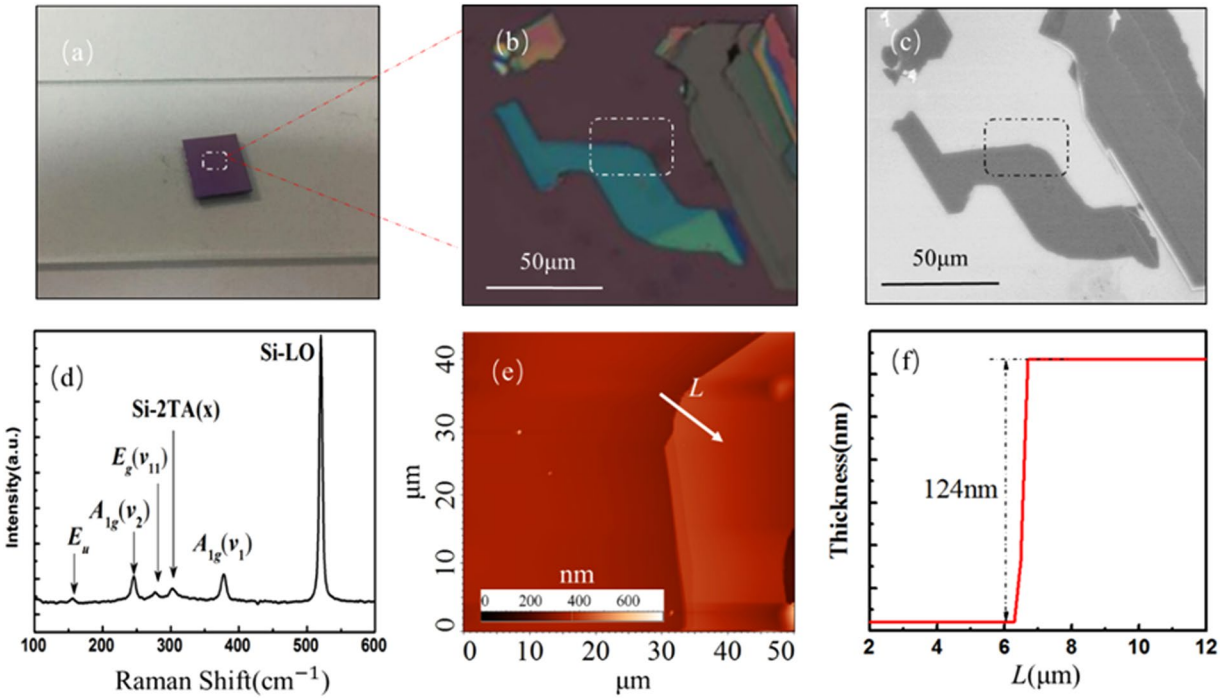

Figure 2. (**a**) The optical image of the $FePS_3$ sample on the surface of substrate. (**b**) The optical microscope image of sample $FePS_3$ prepared by mechanical exfoliation method. (**c**) The SEM image of sample. (**d**) The Raman spectrum of the $FePS_3$ showing E_u, $A_{1g}(v_2)$, $E_g(v_{11})$, *Si-2TA(x)*, $A_{1g}(v_1)$ and *Si-LO* peaks. (**e**) The AFM image of partial sample circled by white dotted line in (**b**); (**f**)The change of thickness along the white arrow line in the arrowed direction in (**e**).

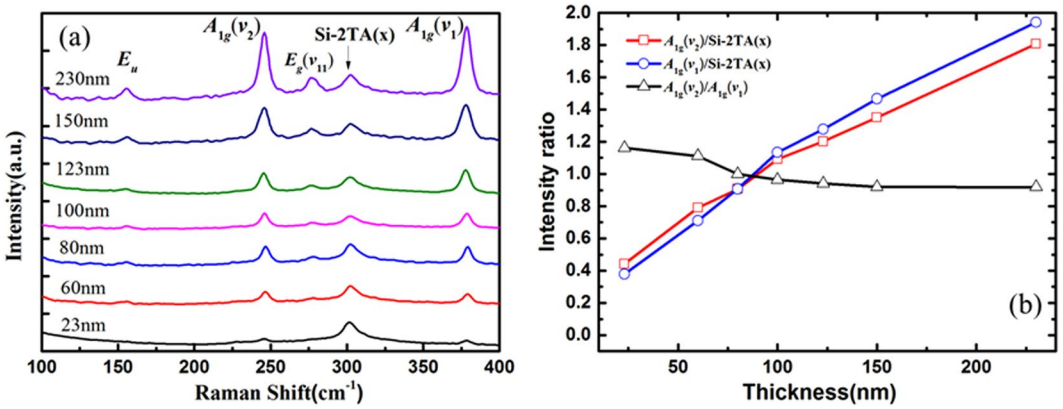

Figure 3. (**a**) The Raman spectrum of $FePS_3$ with different thicknesses. (**b**) The change of intensity ratio of characteristic peaks with increasing thickness.

intensity ratio remains declining gradually as the thickness increases from 100 nm. When the thickness is 230 nm, the intensity ratio is approximately 0.918. It could be understood that the out of plane vibration modes on the contribution of Raman peaks tend to be unchanged as the thickness of sample is increasing. In addition, when the thickness is below 80 nm, the intensity ratio of the $A_{1g}(v_2)$ peak to the *Si-2TA(x)* peak is greater than the intensity ratio of the $A_{1g}(v_1)$ peak to the *Si-2TA(x)* peak. As the thickness increases, the values of E_u, $A_{1g}(v_2)$, $E_g(v_{11})$, and $A_{1g}(v_1)$ with respect to Si-LO peaks remain increasing without exception. These results demonstrate that the Raman spectra of the $FePS_3$ samples with different thickness have diverse characteristics, which apply a platform to study the characteristics of $FePS_3$ during Ga^+ ion irradiation by analyzing the Raman spectra. Figure 4(a,b) is the AFM image of sample S1 before and after Ga^+ irradiation, which demonstrates that the thickness of sample S1 is obviously thinned. That could also be observed in its optical images (shown in Fig. 4(c,d)). The height profile along line in Fig. 4(e) suggests that the lateral distance of obtained sample S1 is measured to be ~23 nm. After irradiation, the thickness of S1 is measured to be dropped by 4 nm with 30 μs irradiation and 5 nm with 40 μs irradiation, respectively. Figure 5 is the AFM and optical images of sample S2 before and after Ga^+ irradiation. The

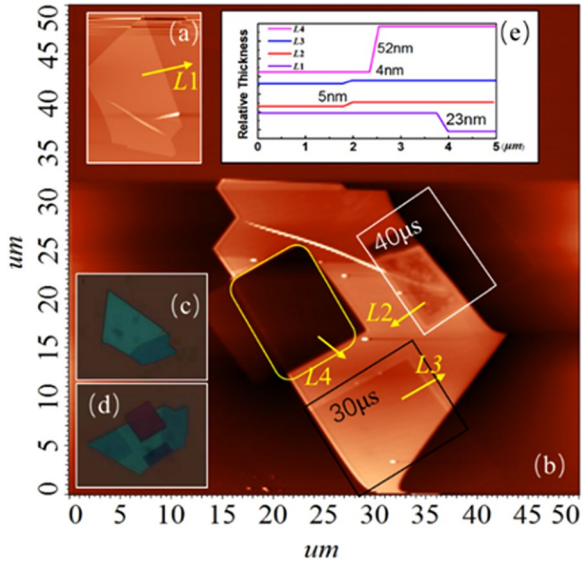

Figure 4. The AFM and optical images of $FePS_3$ sample with thicknesses of 23 nm (S1): (**a**) The AFM image of sample S1 before irradiation. (**b**) The AFM image of sample S1 after irradiation. (**c**) The optical image of sample S1 before irradiation. (**d**) The optical image of sample S1 after irradiation. **(e)** The change of thickness along the yellow arrow line in the direction of the arrow.

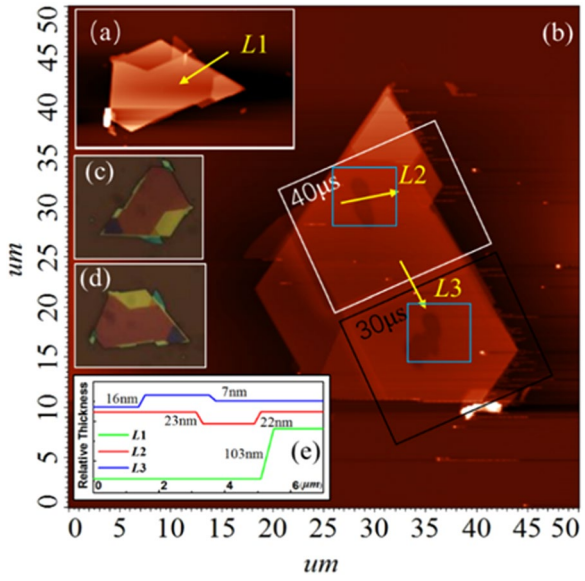

Figure 5. The AFM and optical images of $FePS_3$ sample with thicknesses of 103 nm (S2): (**a**) The AFM image of sample S2 before irradiation. (**b**) The AFM image of sample S2 after irradiation. (**c**,**d**) The optical image of sample S2 before and after irradiation. (**e**) The change of thickness along the yellow arrow line in the direction of the arrow.

thickness of sample S2 is ~103 nm shown in Fig. 5(e). As shown in Fig. 5(a,b), the thickness of S2 is also thinned after Ga^+ irradiation (~16 nm for 30 μs irradiation and ~22 nm for 40 μs irradiation). The optical images of S2 before and after Ga^+ irradiation is shown in Fig. 5(c,d). Note that we find the rate of radiation-induced thinning is a little bit of change for $FePS_3$ samples with different thicknesses. Considering the FIB equipment used in our experiment, it could be understood as follows: (1) due to the $FePS_3$ sample with different thickness is obtained by using mechanical exfoliation method. The effective area of $FePS_3$ with desired thickness is different. Generally, the thicker sample has a large effective area while thinner sample owns a smaller effective area. When using Ga^+ ions beam to irradiate the surface of $FePS_3$ samples, because it is difficult to place the material in the center of the Ga^+ ions beam spot, which affects the rate of radiation-induced thinning. (2) Since the Ga^+ ions beam has a fast irradiation rate, as for thinner samples, the precise focus under Ga^+ ions imaging is hard. Therefore, there has a tradeoff between focus level and thinning rate. As a result, the rate of radiation-induced thinning for different samples might be a little different.

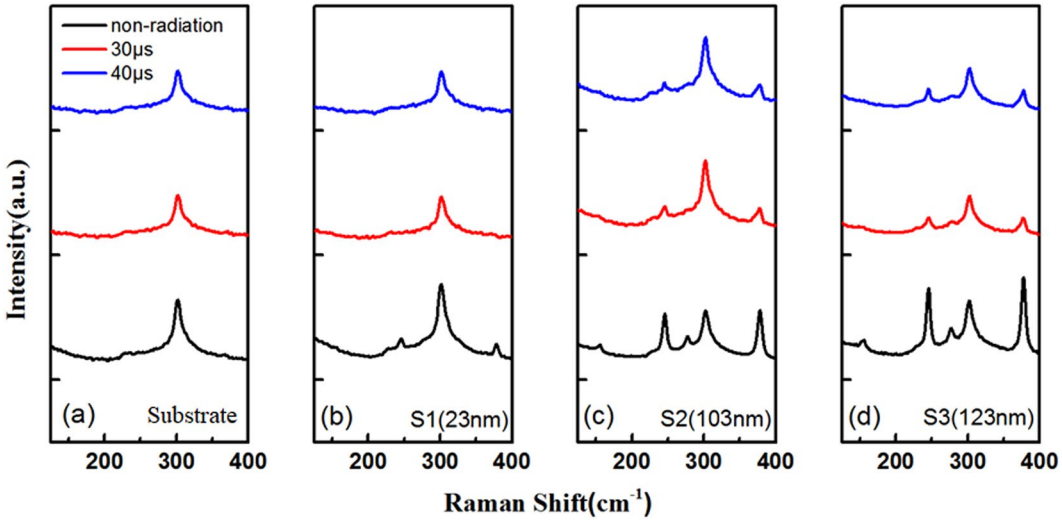

Figure 6. The Raman spectrum of $FePS_3$ samples before and after Ga^+ ion irradiation. (**a**) substrate; (**b**) S1; (**c**) S2; (**d**) S3.

Sample	Time(μs)	$A_{1g}(v_2)$/Si-2TA(x)	$A_{1g}(v_1)$/ Si-2TA(x)	$A_{1g}(v_2)/A_{1g}(v_1)$
S2	0	0.958	1.005	0.953
	30	0.520	0.507	1.025
	40	0.505	0.487	1.038
S3	0	1.154	1.277	0.904
	30	0.630	0.614	1.026
	40	0.626	0.598	1.046

Table 1. The intensity ratio of characteristic peaks of sample S2 and S3 following different irradiation times.

Discussion

Figure 6(a–d) are the Raman spectra of the substrate, sample S1, S2 and S3 (123 nm) before and after the Ga + ion irradiation, respectively. Due to the thin thickness of S1, the Eu peak and the Eg(v_{11}) peak are not present in the Raman spectrum before irradiation, and all the characteristic peaks disappear in the normalized Raman spectra after irradiation. For sample S2, the E_u peak corresponding to the out-of-plane vibration of two $[P_2S_6]^{4-}$ units in adjacent layers and the Eg(v_{11}) peak corresponding to tangential vibration of the P-P bands and in-plane vibration of $[P_2S_6]^{4-}$ unit disappeared in the Raman spectrum after Ga + ion irradiation. The intensity of $A_{1g}(v_2)$ and $A_{1g}(v_1)$ peaks corresponding to stretching vibration of the P-P bands and out-of-plane vibration of two $[P_2S_6]^{4-}$ unit weakened to some extent. Table 1 shows the intensity ratio of characteristic peaks of sample S2 and S3. For sample S2, when the irradiation time is 30 μs, the intensity ratio of the A_{1g} (v_2) peak with respect to the Si-2TA(x) peak is 0.520, which is 0.438 lower than that of the non-irradiated sample. The intensity ratio of the A_{1g} (v_1) peak with respect to the *Si-2TA(x)* peak is 0.507, which is 0.498 lower than that of the non-irradiated sample. The intensity ratio of A_{1g} (v_2) peak with respect to A_{1g} (v_1) peak is 1.025, which is 0.072 higher than that of the non-irradiated sample. When the irradiation time is 40 μs, the value of A_{1g} (v_2) peak to *Si-2TA(x)* peak, A_{1g} (v_1) peak to *Si-2TA(x)* peak, and A_{1g} (v_2) peak to A_{1g} (v_1) peak are 0.505, 0.487, and 1.038, respectively. For sample S3, the change of intensity ratio is similar to that of S2 after irradiation. The results indicate that the intensity ratio of the $A_{1g}(v_1)$ peak and the *Si-2TA(x)* peak decreases as the irradiation time increases and the intensity ratio of the $A_{1g}(v_2)$ peak and the *Si-2TA(x)* peak also decreases, but the change of intensity ratio of the $A_{1g}(v_2)$ and $A_{1g}(v_1)$ peaks is opposite. The change of peaks in the Raman spectra are due to the damage of the bipyramid structure of $[P_2S_6]^{4-}$ units because of the cleavage of the P-P bands and the P-S bands during Ga^+ ion irradiation.

In summary, the effect of the Ga^+ ion beam irradiation on multilayer $FePS_3$ is systematically investigated with diverse irradiation times. The corresponding relation between the thickness of samples and the intensity ratios of characteristic active peaks is obtained by analyzing Raman spectrum. The thickness of samples before and after the Ga^+ ion beam irradiation is measured by AFM, which shows that the samples irradiated by Ga^+ ion beam became slightly thinner. The thickness of the sample irradiated by Ga^+ ion beams was obtained by calculating the intensity ratio of A_{1g} (v_2) peak and A_{1g} (v_1) peak, which is close to the thickness of it directly measured by AFM. Finally, compared with the un-irradiated sample with the same thickness, the E_u peak and $E_g(v_{11})$ peak disappeared after irradiation, indicating that the Ga^+ ion irradiation could affect the surface structure of the sample. The peaks disappeared in the Raman spectrum are attributed to the attenuation of vibration mode due to the damage of bipyramid structure of $[P_2S_6]^{4-}$ units and the cleavage of the P-P bands and the P-S bands during Ga^+ ion irradiation. Due to the bandgap of $FePS_3$ is related to the

layer numbers, the material properties (such as electrical properties and nonlinear optical properties) of $FePS_3$ might be engineered by Ga^+ ions irradiation. The results are of vital importance for engineering the structural and optical characteristics of $FePS_3$ by Ga^+ ion beam irradiation.

Methods

An optical microscopy (BX41M-LED, Olympus), a Raman spectroscopy (Senterra, Bruker), an atomic force microscopy (NT-MDT Solver SPM &SNOM) and a scanning electron microscope (HITACHI-4800) are employed to characterize the materials properties. A focused ion beam system (FIB, FEI Helios-600i) is utilized to irradiate the $FePS_3$ samples with Ga^+ ion beam.

Received: 13 May 2019; Accepted: 4 October 2019;
Published online: 23 October 2019

References

1. Xia, F. *et al*. Two-dimensional material nanophotonics. *Nature Photonics* **8**(12), 899 (2014).
2. Xu, M. *et al*. Graphene-like two-dimensional materials. *Chemical reviews* **113**(5), 3766–3798 (2013).
3. Bhimanapati, G. R. *et al*. Recent advances in two-dimensional materials beyond graphene. *ACS nano* **9**(12), 11509–11539 (2015).
4. Wang, Q. H. *et al*. Electronics and optoelectronics of two-dimensional transition metal dichalcogenides. *Nature nanotechnology* **7**(11), 699 (2012).
5. Kurosawa, K., Saito, S. & Yamaguchi, Y. Neutron diffraction study on $MnPS_3$ and $FePS_3$. *Journal of the Physical Society of Japan* **52**(11), 3919–3926 (1983).
6. Lee, J. U. *et al*. Ising-type magnetic ordering in atomically thin $FePS_3$. *Nano letters* **16**(12), 7433–7438 (2016).
7. Ressouche, E. *et al*. Magnetoelectric $MnPS_3$ as a candidate for ferrotoroidicity. *Physical Review B* **82**(10), 100408 (2010).
8. Gusmão, R., Sofer, Z. & Pumera, M. Exfoliated Layered Manganese Trichalcogenide Phosphite ($MnPX_3$, X = S, Se) as Electrocatalytic van der Waals Materials for Hydrogen Evolution. *Advanced Functional Materials* **29**(2), 1805975 (2019).
9. Cheng, Z. *et al*. High-Yield Production of Monolayer $FePS_3$ Quantum Sheets via Chemical Exfoliation for Efficient Photocatalytic Hydrogen Evolution. *Advanced Materials* **30**(26), 1707433 (2018).
10. Schwestka, J. *et al*. A versatile ion beam spectrometer for studies of ion interaction with 2D materials. *Review of Scientific Instruments* **89**(8), 085101 (2018).
11. Wang, Q. *et al*. Effects of Ga ion-beam irradiation on monolayer graphene. *Applied Physics Letters* **103**(7), 073501 (2013).
12. Sharma, P. A. *et al*. Ion beam modification of topological insulator bismuth selenide. *Applied Physics Letters* **105**(24), 242106 (2014).
13. Walker, R. C., Shi, T., Jariwala, B., Jovanovic, I. & Robinson, J. A. Stability of the tungsten diselenide and silicon carbide heterostructure against high energy proton exposure. *Applied Physics Letters* **111**(14), 143104 (2017).
14. Tan, Y. *et al*. Tailoring nonlinear optical properties of Bi_2Se_3 through ion irradiation. *Scientific reports* **6**, 21799 (2016).
15. Li, Z. & Chen, F. Ion beam modification of two-dimensional materials: Characterization, properties, and applications. *Applied Physics Reviews* **4**(1), 011103 (2017).
16. Tsukagoshi, A. *et al*. Spectroscopic characterization of ion-irradiated multi-layer graphenes. *Nuclear Instruments and Methods in Physics Research Section B: Beam Interactions with Materials and Atoms* **315**, 64–67 (2013).
17. Archanjo, B. S. *et al*. The use of a Ga^+ focused ion beam to modify graphene for device applications. *Nanotechnology* **23**(25), 255305 (2012).
18. Buchowicz, G. *et al*. Correlation between structure and electrical transport in ion-irradiated graphene grown on Cu foils. *Applied Physics Letters* **98**(3), 032102 (2012).
19. Wang, Q., Shao, Y., Ge, D., Yang, Q. & Ren, N. Surface modification of multilayer graphene using Ga ion irradiation. *Journal of Applied Physics* **117**(16), 165303 (2015).
20. Gao, Y. *et al*. Bias-switchable negative and positive photoconductivity in 2D $FePS_3$ ultraviolet photodetectors. *Nanotechnology* **29**(24), 244001 (2018).
21. Murayama, C. *et al*. Crystallographic features related to a van der Waals coupling in the layered chalcogenide $FePS_3$. *Journal of Applied Physics* **120**(14), 142114 (2016).
22. Kuo, C. T. *et al*. Exfoliation and Raman spectroscopic fingerprint of few-layer $NiPS_3$ van der Waals crystals. *Scientific reports* **6**, 20904 (2016).
23. Wang, X. *et al*. Raman spectroscopy of atomically thin two-dimensional magnetic iron phosphorus trisulfide ($FePS_3$) crystals. *2D Materials* **3**(3), 031009 (2016).

Acknowledgements

This research was funded by the Foundation of NUDT, grant number JC13-02-13, ZK17-03-01, the Hunan Provincial Natural Science Foundation of China, grant number 13JJ3001, and the Program for New Century Excellent Talents in University, grant number NCET-12-0142.

Author contributions

J.Y. designed the work. H.X. and H.C. performed the experiments. H.X., H.C. and J.Y. wrote the paper. H.X. fabricated the $FePS_3$ samples. H.X., S.W. and J.O.Y. measured the property of $FePS_3$. X.H. performed the experiment of FIB irradiation process. X.H., Y.L. and J.Y. carried out the data analysis. Y.L. and R.C. contributed to the scientific discussion. All authors discussed the results and substantially contributed to the manuscript.

Competing interests

The authors declare no competing interests.

Additional information

Correspondence and requests for materials should be addressed to J.Y.

Reprints and permissions information is available at www.nature.com/reprints.

Publisher's note Springer Nature remains neutral with regard to jurisdictional claims in published maps and institutional affiliations.